Journal of Imaging Science and Technology® 51(3): 225–234, 2007.

On the Mechanism of Phthalazine Toner Chemistry in Controlling Silver Nanoparticle Growth in Photothermographic Imaging Films

S. Chen, B. J. Stwertka and P. J. Cowdery-Corvan
Eastman Kodak Company, 1999 Lake Avenue, Rochester, New York 14650-2157
E-mail: Samuel.chen@kodak.com

D. R. Whitcomb and L. P. Burleva
Eastman Kodak Company, 1 Imation Way, Oakdale, Minnesota 55128

Abstract. *A combination of normal Raman spectroscopy, surface-enhanced Raman scattering spectroscopy, and transmission electron microscopy has been used to demonstrate that phthalazine is the predominant species on the surface of metallic silver nanoparticles in the image at the final stage of development in photothermographic films. Evidence for a small amount of a cotoner, 4-methylphthalic acid, as Ag_2(4-MPA), has also been found. In addition, the organic components around the developed Ag^0 nanoparticles have been directly observed by transmission electron microscopy using RuO_4 staining techniques. A model system, based on interaction between the toner chemicals with nanoparticulate Ag dispersions, has shown that PHZ can directly cause Ag nanoparticles to aggregate but not coalesce. Based on these results, phthalazine adsorption is proposed to play a major role, and the phthalic acid component a lesser role, in controlling metallic silver formation of the preferred metallic silver dendritic morphology. © 2007 Society for Imaging Science and Technology.*
[DOI: 10.2352/J.ImagingSci.Technol.(2007)51:3(225)]

INTRODUCTION

Thermally developed imaging materials based on silver carboxylates have been commercially available for over 40 years.[1,2] The initial success of "dry silver" products can be directly attributed to the simplicity of development, which only involves a heating step (to ~120°C for 10–20 sec). No wet processing is required. Major advances in the technology enabled extremely high-quality images to be printed virtually anywhere. Only a data link and electricity are needed. Consequently, the introduction of the DryView laser imaging system to the medical x-ray film market in 1995 was extraordinarily successful, and over 35,000 imagers for that product have been sold since. Considering this success and the inevitable competition it provoked, it is somewhat surprising how little has been published on the fundamental understanding of the imaging processes.[1–7] Only in the past few years have publications addressed the important mechanisms that form the basis of this imaging technology.[8–12] For example, the most preferred size and shape of the metallic silver in the image was only recently demonstrated to be the "dendritic" form.[13,14] In this case, the dendrites consist of 10–30 extremely fine (5–30 nm diameter) but polydispersed sizes of nanoparticle metallic silver with a minimum aggregation size in the 50–200 nm diameter range, depending on the aggregate shape. Filaments, on the other hand, are an inefficient use of silver for optimum optical density and tone. Now that the optimum metallic silver morphology has been established, the next step in understanding the development process is to determine how the optimum morphology can be produced in preference to other morphologies (such as filaments).

The "toner" component of the typical photothermographic (PTG) formulation is usually a pair of compounds based on phthalazine (PHZ) and phthalic acid (PA) and their derivatives, such as 4-methylphthalic acid (4-MPA), Figure 1. This cotoner pair has been generally considered to produce the desired tone by affecting metallic silver morphology.[1,3,15] However, there is currently no published report that has provided evidence of any compound of any type located on the metallic silver surface at any time in the development process. The objective of this work is to determine exactly what organic compounds are on the growing metallic silver nanoparticle surface in order to determine which one(s) contribute most to the morphology of that particle. With this knowledge, rational design of these compounds should be possible for improved properties such as improved silver efficiency.

While there are numerous techniques for probing the chemical nature of surfaces, few can effectively probe directly within a coated film. For the latter, those can usually only be used on surfaces significantly larger than the nanosized particles that comprise the metallic silver in thermographic imaging materials. However, surface-enhanced Raman scatter-

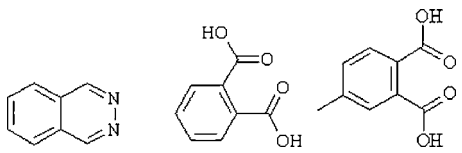

Figure 1. Phthalazine, phthalic acid, 4-methylphthalic acid.

Received Nov. 8, 2006; accepted for publication Feb. 16, 2007.
1062-3701/2007/51(3)/225/10/$20.00.

ing spectroscopy (SERS) is ideally suited for this task. SERS is surface selective, highly sensitive, and is not limited to powder or model systems. In addition, it provides powerful structural information not easily obtained from traditional surface science techniques like electron energy loss spectroscopy or spin polarized electron energy loss spectroscopy.

The SERS phenomenon is a consequence of the coupling between the surface resonance plasmon on nanoparticulate metals with the Raman-active vibrational modes of an adsorbed or adjacent molecule.[16–20] This unique coupling, most commonly observed on copper, silver, and gold, may enhance the vibrational intensities by factors exceeding 10^6. There is an additional enhancement as a result of the bonding of the adsorbate to the SERS substrate, which is often referred to as the "chemical first-layer effect." Extraordinary, "giant" enhancements of 10^{13} have been observed when the SERS substrate fulfills certain morphology requirements.[21] As a result, extremely low levels of chemisorbed compounds can be detected in a matrix containing large quantities of other components not chemisorbed to the metal surface. Consequently, this technique should be directly applicable to the study of organic compounds on the nanoparticulate silver that is generated in the thermal development reaction of photothermographic imaging materials. Of particular interest are the "toners" used in PTG media.

By comparison, transmission electron microscopy (TEM) can usually provide morphology information on the extent and thickness of most materials adsorbed onto the Ag surface. Generally, organic molecules are made up of low atomic number elements (consisting of such atoms as N, C, O, or H, etc.), and these have low electron absorption cross sections. Their resulting contrast in TEM is usually too low to permit them to be differentially detected and analyzed. However, it is sometimes feasible to take advantage of the fact that local deposits of organic compounds with available bonding ligands, such as the nitrogen-based azine group on the PHZ, can react with heavier atomic numbered metals, so that the resulting metallo-organic adduct can produce a darker contrast from such local regions, and hence reveal the morphology of the original organic species. Staining by transition metals is a sample preparation method often used in the life science and polymer science fields to enhance the electron contrast of otherwise electron-transparent organic materials.[22,23] Once detected, the resolution of a TEM can be applied to determine the morphologies of the organics at the submicrometer, or even nanometer, size level. For the work reported here, RuO_4 vapor, generated from $RuCl_4$ with $HClO_2$ (as found in the commercial bleach "Clorox"), was used to stain the microtomed film sections, and the optimum contrast was experimentally found by varying the staining time. RuO_4 is considered a nonspecific staining reagent, i.e., capable of reacting with most organic ligand groups. It is used here as our first attempt to identify the potential of such a technique to directly elucidate the location and morphology of key organic components in PTG media. Since photothermographic constructions normally contain PHZ, the possibility of identifying and directly imaging this species seemed reasonable.

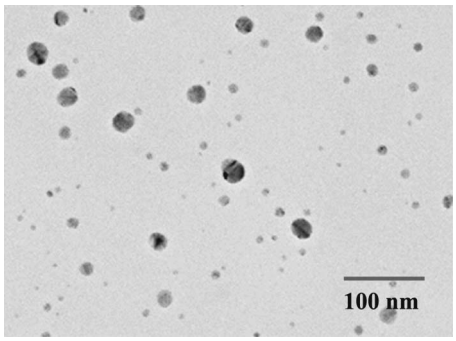

Figure 2. Silver nanosol dispersed in gelatin. Note the polydispersity (5–40 nm) of the well-separated, individual Ag nanoparticles.

It has been suggested that the role of the toner in a direct thermographic imaging construction is to promote the aggregation of isolated silver nanoparticles.[24,25] Photothermographic formulations are complex, multicomponent systems. Possible synergistic effects make it difficult to use the complete photothermographic formulation for probing the role of each component. A complementary approach for investigating the effect of toners on isolated Ag nanoparticles is to use a simpler system based on a dispersion of discrete Ag nanoparticles, similar to that of the original Carey Lea silver (CLS)[†]. Such an emulsion of Ag nanoparticles stabilized in gelatin was prepared, and various toner solutions were added, thermally processed, and any changes to the resulting solutions were investigated. The starting silver nanosol solution was also imaged by TEM and found to be a polydispersed distribution of nanoparticulate Ag, Fig. 2. The size of the individual particles in this nanosol (5–40 nm) is similar to the constituent Ag nanoparticles in directly developed thermographic film,[14] as well as the dendrites observed in photothermographic films.[13] The effect of a series of toner solutions on the silver nanosol was characterized by TEM, SERS, and visual inspection.

Using a combination of Raman spectroscopy and electron microscopy, we have now been able to demonstrate that phthalazine is the predominant species on the surface of the metallic silver nanoparticles in the image at the final stage of imaging in photothermographic films. Even though phthalic acid is part of the "toner package," phthalazine is the primary component observed on the silver nanoparticle surface at this stage of the imaging process. The organics around the developed Ag^0 nanoparticles have also been directly detected by transmission electron microscopy using an RuO_4 stain. Based on these results, phthalazine adsorption is proposed to play a major role in controlling metallic silver formation of the dendrites.

[†]The Ag nanoparticulate dispersion used here, stabilized in gelatin, which should not be confused with the original preparation of CLS,[26] the product of silver nitrate reduced with ferrous citrate. Both processes produce similar silver nanospheres, approximately 5–3 nm in diameter. A key feature of both of these silver nanosols is that they are individual particles and not agglomerated in any way (see Figure 2). The term CLS is commonly used to describe this type of silver nanoparticulate dispersion.

EXPERIMENTAL

Photothermographic Coatings

A photothermographic formulation typical for these materials was used in this investigation, as described previously.[27] Our previous investigations[13] showed that the temperature and time of photothermographic processing affect the morphology of the imaged silver particles. The standard formulation coating, PTG-1, was exposed with a laser sensitometer incorporating an 810 nm laser diode and was thermally processed at standard conditions (122°C/15 sec).

The modified photothermographic film without the infrared sensitizer, PTG-2, was exposed to a Xe discharge lamp pulse and thermally processed at the same processing conditions as the standard material (122°C/15 sec). The area with $D_{max}=3.28$ (maximum optical density) was used for further PTG-2 study.

The modified photothermographic films without the toner, PHZ, or co-toner, 4-MPA, were the normal formulation with these components selectively left out, PTG-3 and PTG-4, respectively, and processed similar to that of PTG-1.

Silver Nanosol Preparation

Silver nanosol samples were prepared by the reduction of silver nitrate with dextrine, as a 5 wt. % dispersion, and stabilized in gelatin. A sample of 0.32 g of the nanosol was heated gently and mixed with 5 mL of deionized, distilled water. This served as the "stock" silver nanosol solution. Equal volumes of the stock solution and 0.02 M solutions of various toners were mixed in a glass vial. Several drops of this mixture were placed on a glass slide, which was heated on a laboratory hot plate (setting "2") until the solvent evaporated. Several of the toners were not soluble in acetone, methanol, or water. In these cases, a dispersion of the toner was added to the nanosol solution, and the mixture heated as described above. In these cases, the total toner was obviously much higher than the cases of soluble toners, but the solution concentration was unknown.

Model Compounds

Ag_2(4-MPA) was prepared by stoichiometric metathetical exchange of Ag^+ for Na^+ on the phthalate anion in water. Washing and drying produced a white powder that is insoluble in most solvents. Attempts to prepare the 1:1 complex, AgH(4-MPA), for comparison purposes, only yielded Ag_2(4-MPA) (by elemental analysis).

Raman Spectroscopy

Micro Raman spectra were collected with a JY Horiba LabRam at 180° backscatter with an MSPlan 100X objective, mounted in an Olympus 40XB microscope. The spot size was approximately 2 μm in diameter, and 8–10 μm in thickness (Z-direction). The excitation wavelength was 514 nm, 633 nm, or 785 nm, as appropriate. The power of the unfiltered laser was about 250 mW. Neutral density filters were used to decrease the laser power until it was determined that the laser was not damaging the sample. The power used depended on the sample and the laser wavelength. Typically, film samples were probed with 785 nm excitation at 2.5 mW.

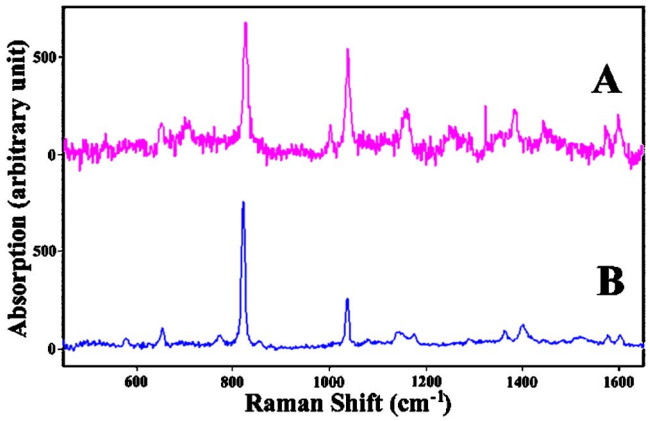

Figure 3. Raman spectral data for a full formulation photothermographic film. (A) SER-spectrum of the D_{max} region of a photothermographic film, $\lambda_{exc}=633$ nm. (B) Normal Raman (NR) spectrum of PHZ powder, $\lambda_{exc}=785$ nm.

Transmission Electron Microscopy

The microstructures of photothermographic films were examined by transmission electron microscopy. Film cross sections were prepared in a Leica Ultracut S microtome using a diamond knife, and thin sections were wet-transferred onto a carbon-coated Cu grid. All electron beam imaging and analysis were gathered with the sample kept at liquid nitrogen temperature in a JEM-2000FX instrument. For RuO_4 staining experiments, the microtomed cross-sections of photothermographic media were cut to a thickness of ~60 nm, which was estimated based on their reflected color,[28] and exposed to the heavy metal oxide vapor. Our experience indicated that various staining times were needed to find the optimum condition necessary to image both the core dendrite and the organic shell. Insufficient stain failed to reveal the shell, while extended staining times usually resulted in too dark a contrast that often covered up the dendrite's fine structures.

RESULTS

Recent evidence suggests that the nanoparticulate Ag in thermographic formulations can serve as a suitable SERS substrate for probing organic compounds in close proximity to that silver.[29] In Figure 3, Raman spectral data demonstrate that PHZ is the predominant organic species on the surface of the imaged silver in the Dmax region in a full-formulation photothermographic film (PTG-1, Table I). It is important to note that this is not a model system. The data demonstrate that this technique is directly applicable to *in situ* investigation of actual imaging films. Trace A is a SERS spectrum of that photothermographic film and trace B is the normal Raman spectrum of PHZ powder. All of the Raman bands in trace A are accounted for and can be attributed to PHZ.

We previously demonstrated that most of the silver complexes detected in direct thermal films experienced degradation at Raman excitation wavelengths that were shorter than 785 nm.[29] It has also been reported in the literature that PHZ adsorbed onto a silver SERS substrate decom-

Table I. Photothermographic materials processed at different temperature and development time conditions.

ID	Sample	Temp (°C)	Time (sec)	D_{min}	D_{max}
1	**Control, PTG-1**	**122**	**15**	**0.221**	**3.745**
2	No_PHZ, PTG-3	122	15	0.22	0.229
3	No_4MPA, PTG-4	122	15	0.22	0.231
4	**Control, PTG-1**	**145**	**35**	**2.007**	**3.716**
5	No_PHZ, PTG-3	145	35	0.253	0.263
6	No_4MPA, PTG-4	145	35	0.240	0.252
7	**Control, PTG-1**	**165**	**35**	**4.210**	**5.022**
8	No_PHZ, PTG-3	165	35	0.270	0.344
9	No_4MPA, PTG-4	165	35	4.369	5.344

poses, even when 633 nm laser excitation is used.[30] The full photothermographic formulation imaging layer, PTG-1, contains an infrared adsorbing dye (λ_{max}=810 nm in the film), which strongly adsorbs 785 nm light. Consequently, the Raman spectrum of photothermographic formulation cannot be collected using 785 nm laser excitation, where less PHZ decomposition would occur (compared to when the data is collected using 633 nm excitation). Hence trace A (in Fig. 3), collected with 633 nm excitation, represents the best spectrum of the complete photothermographic formulations possible, using the available instrumentation.

From the SERS data, PHZ is clearly the dominant species in the imaged film. However, it is important to attempt the observation of other organic formulation components present at lower concentrations than PHZ (or slightly farther away from the silver surface). Therefore, longer wavelength laser excitation is necessary in order to minimize the degradation of any silver:organic adducts that are formed at the surface of the imaged silver. A slightly modified photothermographic formulation, PTG-2, containing everything except the infrared dye, was prepared and imaged by exposure to a Xe white light source and thermally processed similar to PTG-1. Trace A in Figure 4 represents a typical spectrum (785 nm excitation) of the imaged IR dye-free photothermographic film at D_{max}.

It can be seen that PHZ still dominates the SER spectrum, indicating that this toner is the predominant species present on the silver surface. In addition to the bands attributed to PHZ, there are two bands (675 cm^{-1} and 832 cm^{-1}) that may be attributed to Ag_2(4-MPA). It is important to note that these bands were very sensitive to laser irradiation during the course of data collection. They were never observed when 633 nm laser irradiation was used, and they also diminished or disappeared during long collection times using 785 nm excitation, so care must be taken in their interpretation. In order to confirm the presence of Ag_2(4-MPA) it would be necessary to repeat the measurements with very careful attention to exposure of the samples to laser excitation (laser power and collection time). It would also be prudent to attempt the same series of measurements using laser excitation even further into the infrared. These

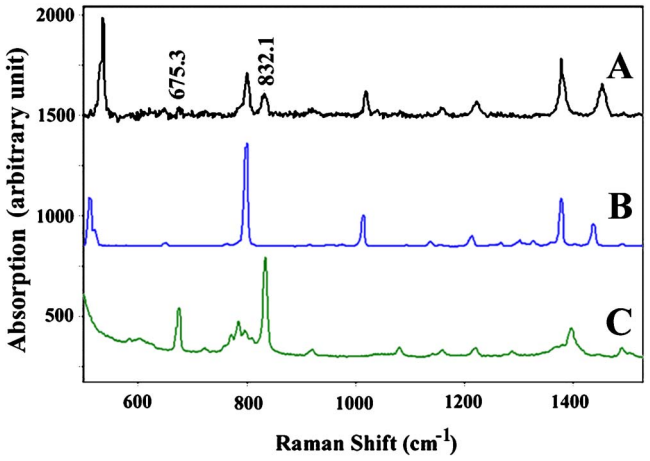

Figure 4. (A) SER spectrum of a photothermographic film without an IR sensitizing dye; (B) NR spectrum of PHZ powder; (C) NR spectrum of Ag_2(4-MPA) powder.

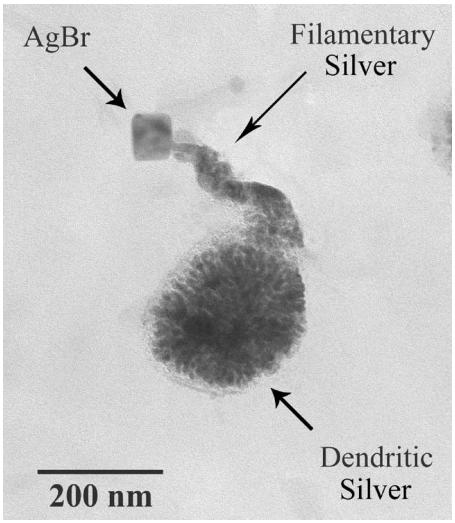

Figure 5. TEM image of developed Ag in photothermographic media.

experiments would be particularly useful in conjunction with TEM. It might then be possible to determine the preference of particular compounds for particular silver morphologies (dendrites or filaments). The spectroscopic data suggests that PHZ passivates the dendritic silver nanostructures within the imaged film. A special application of a TEM staining technique provides additional support for this conclusion.

Previously, it was shown that the reduction of silver carboxylate in a photothermographic media resulted in the formation of a unique combination of metallic silver forms, which are the fundamental imaging elements in a PTG film.[13] It consists of a combination of filamentary and dendritic Ag, with the former usually attached to a AgBr grain on which the latent image was originally formed during the exposure process, Figures. 5 and 6(a).

The dendritic Ag is now known to be a spherical aggregate of many nanosized Ag crystallites, formed in proximity to each other, Fig. 6(b). Its "broccoli head" morphology pro-

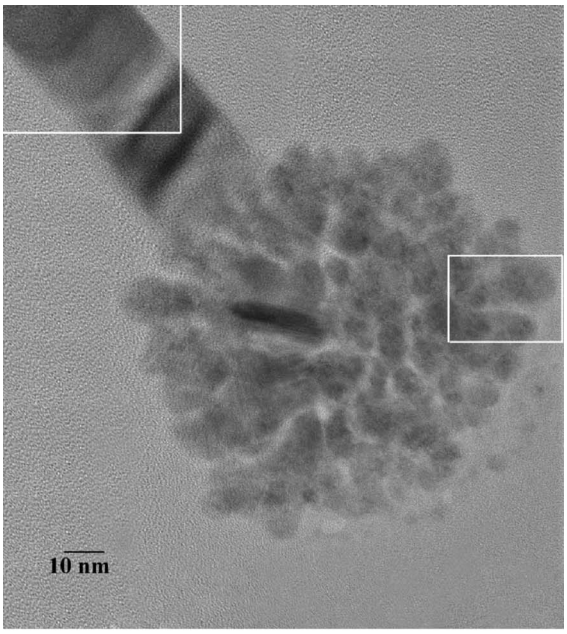

(a)

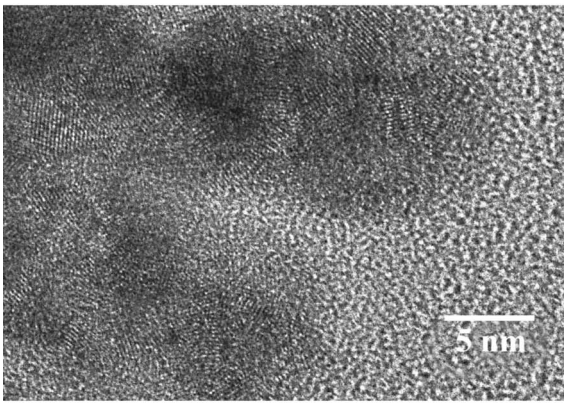

(b)

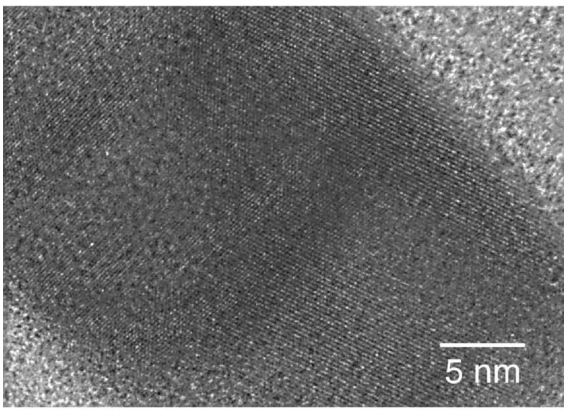

(c)

Figure 6. (a) High magnification image of the developed Ag combination in photothermographic film formulations. The boxed-in areas are enlarged in (b) and (c). (b) High-resolution lattice image of dendritic Ag, showing nanoregions of crystalline Ag in close proximity to each other. (c) High-resolution lattice image of a filamentary Ag, showing the relatively long-range structural order across the entire width of the filament.

vides a large surface area-to-mass ratio and represents a highly efficient form of Ag for the purpose of light absorption.[14] By contrast, the filamentary silver is usually a single strand of crystalline silver, made up of multiple twins, Fig. 6(c). By itself, this is not the preferred image element because its lower surface area-to-mass ratio would provide poor covering power and imparts a brown tone which is undesirable.[13]

After exposing a thin microtomed cross-section of photothermographic media for 20 sec to RuO_4 vapor, TEM investigation of the stained components in photothermographic films identified the presence of an organic shell around the developed Ag. However, under these long reaction-time conditions, the stain was found to strongly react with the organic species, and the high contrast shell around the developed silver was easily detectable. Unfortunately, at this high stain level, most of the morphological details associated with the "broccoli-like" structure of the dendritic Ag became obscured. Interestingly, an organic shell around the AgBr or the filamentary Ag was not clearly seen and suggested that these two features either are not extensively passivated or are not passivated by the same organic component.

In order to compensate for the strong affinity of the RuO_4 vapor for the organic species, the staining conditions were modified. Experimenting with successively shorter exposure times showed that an exposure time of 5 sec was sufficient to reveal the organic shell but not dense enough to obscure the unique broccolilike morphology of the dendritic Ag, Fig. 7(a). Focusing in on these lightly stained features, higher magnification images revealed both the organic shell, as well as the known morphology of the dendritic Ag, thereby directly showing the core-shell relationship between the internal dendritic Ag and the external passivation shell, Fig. 7(b). The thickness of this shell was ~20–30 nm, i.e., significantly more than a monolayer deposit of the organic species. Again, no clear evidence of a detectable layer around the filamentary Ag or the AgBr grain was found. Therefore, coupling this staining data with the SERS information suggests that the PHZ toner plays a major role in passivating the dendritic form of the metallic silver in the photothermographic image.

Additional information about the role of PHZ was obtained using a model system designed to examine the interaction of toners on "simple" silver nanoparticles surfaces. Monodisperse, CLS-like silver nanosol was diluted with water and mixed with toner solutions. The resultant dispersions were characterized by TEM and SERS. Diluted silver nanosol is a pale yellow and transparent solution, which is the result of 5–40 nm sized nanoparticles of Ag, Fig. 2.

The room temperature addition of a dilute solution of PHZ to silver nanosol produced no change to the solution. Upon heating to ~100°C and drying to a film, the yellow color of the nanosol changed to dark green. TEM examination of the green film showed the individual Ag nanoparticles had aggregated, with the majority of the clusters containing a large number of particles (>20), and most were

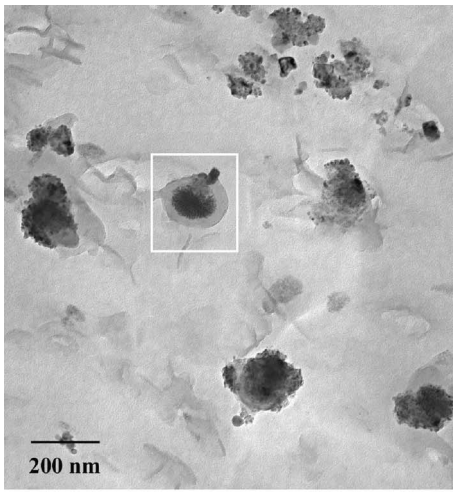

(a)

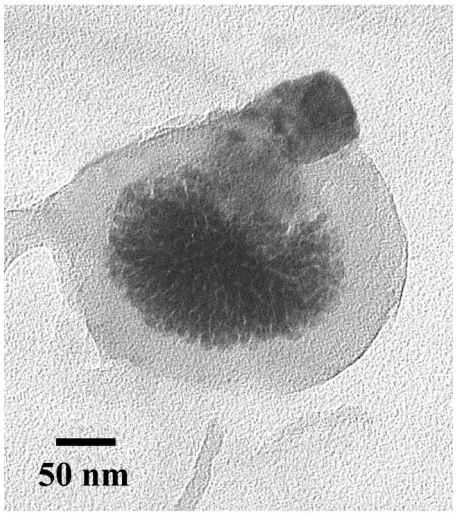

(b)

Figure 7. Lightly stained developed Ag in photothermographic media at (a) lower magnification. The boxed-in area is enlarged in (b) where the higher magnification revealed both the organic passivation shell and the broccoli-like dendritic Ag core.

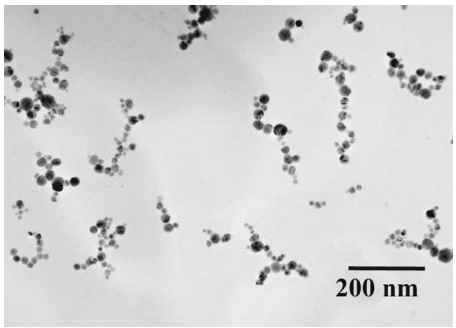

Figure 8. Silver nanosol nanoparticles aggregated with PHZ, visually observed to be dark green.

either linear or branched linear in morphology, Figure 8. Smaller aggregates with <10 particles were less common. The larger aggregates, in excess of 200 nm, should induce a black tone, as these would be expected to absorb light

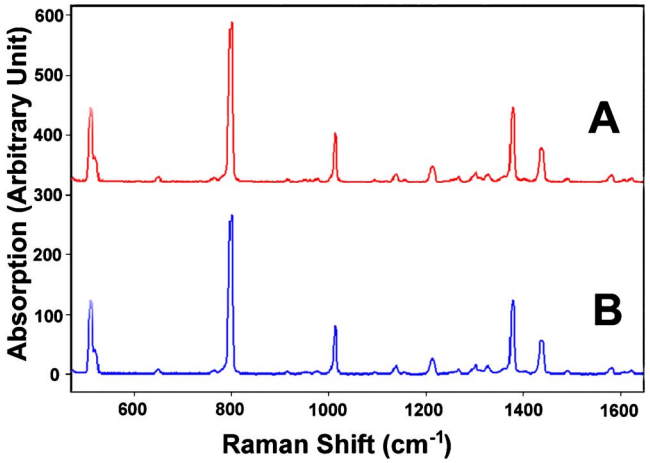

Figure 9. (A) Raman data for PHZ with silver nanosol. SERS spectrum of the film obtained by adding a dispersion of PHZ to silver nanosol, followed by heating. (B) Normal Raman spectrum of PHZ powder. λ_{exc}=785 nm for both spectra.

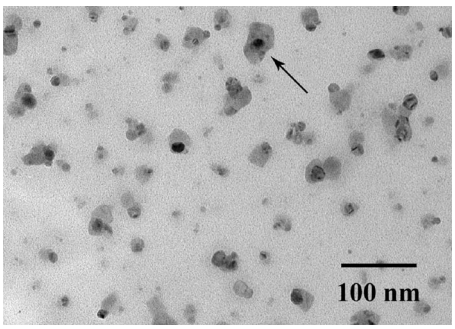

Figure 10. TEM image of RuO_4 stained silver nanosol in gelatin.

throughout the visible spectrum region, while the minority mixture of smaller aggregate sizes (40–100 nm) contribute to the greenish hue. Interestingly, we noted that while these nanoparticles may have come in close contact with each other, they were stable and did not coalescence with each other within the aggregates. The PHZ toner brought the particles together without significantly reducing the surface area:mass ratio of the Ag in the aggregates. In contrast, thermally aggregated CLS (prepared by the original 1889 procedure[26]) processed in polyvinylpyrrolidinone generated Ag particles that not only were aggregated but also significantly coalesced.[14]

The PHZ-aggregated silver nanosol is an excellent SERS substrate, as demonstrated by the significant Raman sensitivity for PHZ in the green films, Figure 9. This is completely consistent with the current understanding on the effect of substrate morphology on the enhancement factor. As discussed above, substrates with fractal-like morphologies result in the largest enhancements.[30] Stockman has described a theoretically ideal substrate morphology to support giant SERS.[31] The TEM of PHZ-aggregated silver nanosol, Fig. 8, demonstrates that morphology empirically.

RuO_4 staining experiments on the yellow silver nanosol and on the dark green nanosol-PHZ dispersions revealed the

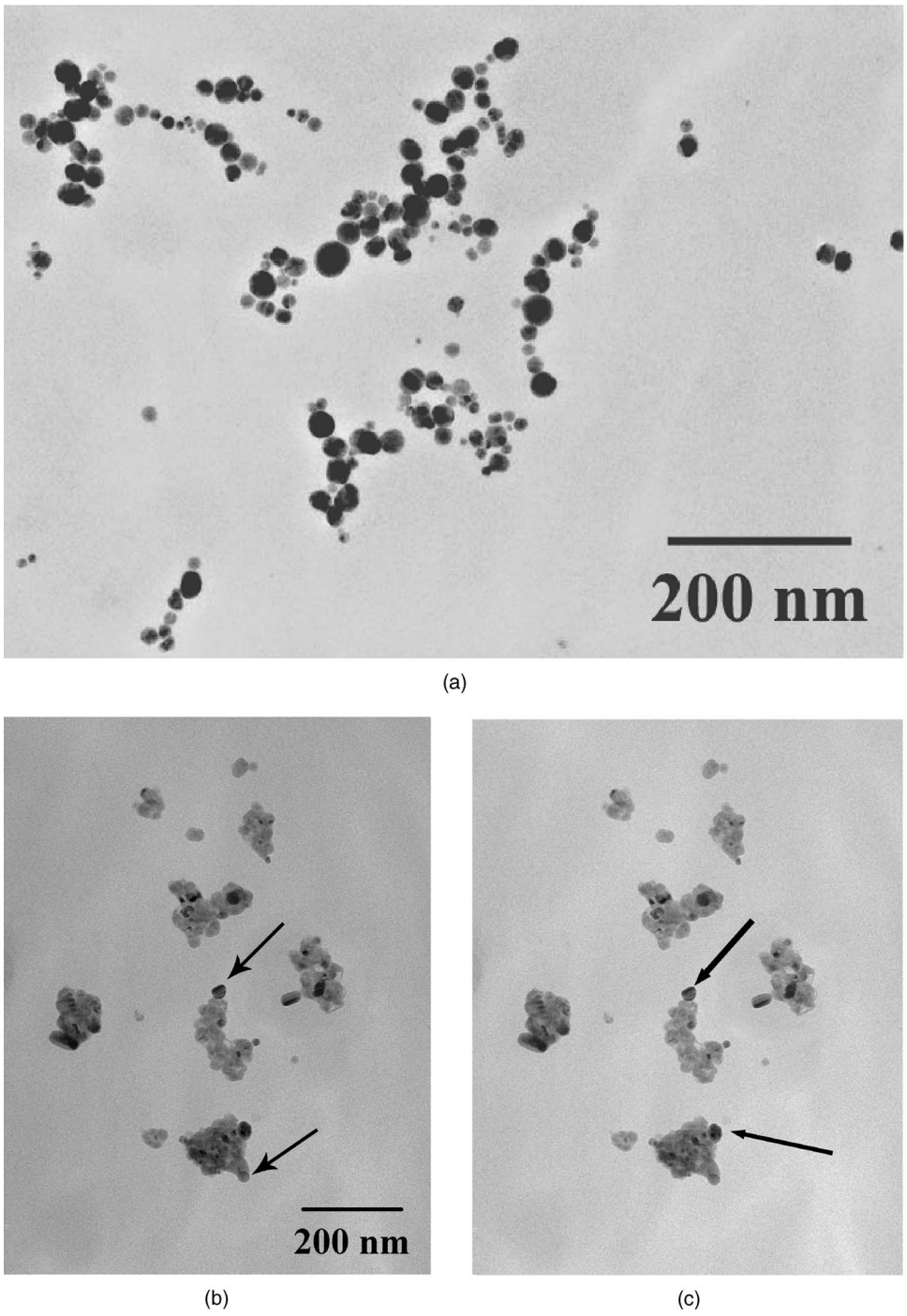

Figure 11. (a) High-magnification TEM view of PHZ on silver nanosol, without staining. Note the aggregate morphology is linear, or branched linear, and the primary nanoparticles remain uncoalesced with its neighboring particles. (b) RuO_4 stained silver nanosol+PHZ. The PHZ toner appears as a thin shell around the Ag aggregates. (b) and (c) are TEM images of the same area of view, except one is tilted 5° to the other, to reveal the location of the Ag particles through diffraction-contrast enhancement. Many particles do not appear to be completely passivated by the organic toner (arrows).

presence of a thin organic shell around these Ag nanoparticles. For the nanosol in gelatin, a thin stained shell was seen around most of the well-dispersed nanoparticles, Figure 10. While the shell thickness varied between particles, most appeared to have at least a thin coating around them.

In the presence of PHZ, however, staining revealed a shell that engulfed most of the Ag aggregates, Figure 11. Some uncoated Ag surfaces were found, suggesting different degrees of passivation between nanoparticles. Since PHZ caused the observed aggregation of Ag particles, this toner must have a higher affinity for the Ag surface than the original gelatin.

The aggregation mechanism for the formation of dendritic silver from small silver nanoparticles has not been es-

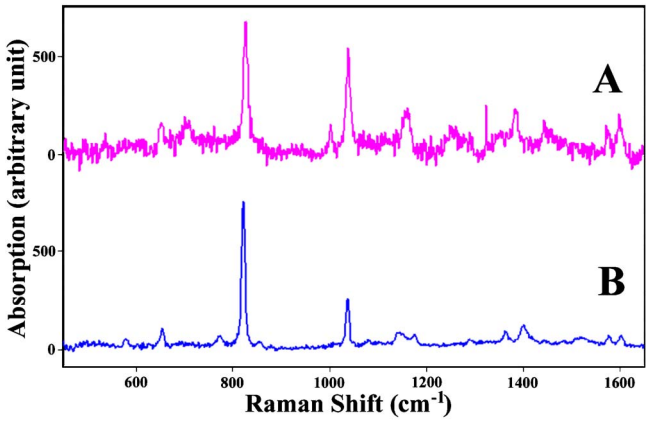

Figure 12. Raman data for PA. (A) SER spectrum of the film obtained by adding a dispersion of PA to silver nanosol, followed by heating. (B) Normal Raman spectrum of PA powder.

tablished and is barely discussed in the PTG literature. One route is the agglomeration of individually formed Ag^0 into the spherical dendrites.[11] However, there are many arrested development studies in the literature, and none have detected significant quantities of preagglomerated particles. Alternatively, supersaturation of silver intermediates might develop the dendrites at the end of the development cycle, as suggested by some arrested development TEMs.[13] In either case, simple electrostatic forces on such high surface-area particles may be sufficient to drive agglomeration. Presumably, the Ag^0 surface is positively charged because excess silver ions arriving at the surface late in the development process do not reduce as the temperature is dropping. It is known that normal silver surfaces under ambient conditions are positively charged.[32,33] Under these conditions, anionic compounds should be suitable stabilizers for colloidal particles, such as proposed previously.[14] Electron-rich donor ligands, such as PHZ, may be reasonable alternatives, which would be consistent with the observed PHZ shell. However, the resulting PHZ shell is apparently not as effective as gelatin in compensating for the charge on the Ag surface because neighboring particles come together to form aggregates. While the mechanism behind such aggregation is not yet clear, the ability to only partially compensate for the charge on the Ag surface, resulting from the reaction by the organic species with Ag surface atoms, is likely the root cause for the aggregation process.

The effect of PA[§] on silver nanosol aggregation was also studied. Unfortunately, the solubility of this acid was insufficient under these circumstances to enable a completely analogous comparison to PHZ. When a slurry of PA was added to the silver nanosol solution, and the mixture was heated, it was difficult to tell by visual examination if a color change had occurred. The resultant film was reddish/orange, and its Raman spectrum contained a strong spectrum, which is assigned to the silver complex, Ag_2PA, Figure 12.

This suggests that PA had adsorbed onto the silver nanosol, causing it to aggregate. TEM analysis was not carried out for the Ag-PA adduct because the dried film could not be redispersed in water to allow a suspension to form, a property necessary for deposition on a TEM grid. The absence of a distinct color change suggests poor aggregation. Increasing the concentration of PA:Ag to force aggregation was not possible because of poor PA solubility. It might be suggested that trace A can be attributed to microcrystalline PA. The major bands in trace A, occurring at the same wavelengths as in the PA reference spectrum (trace B), have different relative intensities. This has been widely observed when comparing SERs spectra (species adsorbed onto Ag) with the normal Raman spectra of the free powder species. Comparison of the color of the films resulting from addition of either PA or PHZ to silver nanosol suggests that PA causes the nanosol to aggregate but to a much lesser extent than PHZ. Even an extremely dilute solution of PHZ will cause a nanosol solution to turn dark green upon heating to dryness. Another explanation for the smaller degree of aggregation caused by PA is mobility. Given that PA is poorly water soluble, the concentration of PA at each silver surface is likely small by comparison to PHZ. The model silver nanosol system has shown an observable interaction between nanoparticulate Ag with PA. The degree of interaction appears small compared to the interaction of silver nanosol with PHZ.

DISCUSSION

Four roles have been identified for the compounds typically described as toners: (1) Silver ion extraction, (2) silver ion transport, (3) silver redox potential modification, and (4) adsorption and control of metallic silver growth.[15] Literature discussion of the chemical role of the toners PA and PHZ in metallic silver formation in PTG materials is very limited. Other than general comments regarding the presumed role in crystal growth,[1–3] or particle aggregation,[24,25] the chemistry related to this question remains generally unexplored. The current consensus regarding the role of the PA component is that it is involved with Ag^+ extraction and possibly transport from the silver soap to the development site [roles (1) and (2)]. The structure of the silver phthalate complex intermediate is claimed to be either an asymmetric silver carboxylate dimer[15] or Ag_2PA[8] (but not the monosilver phthalate). Some evidence for the formation of intermediate silver complexes containing PHZ has been interpreted as support for its role in silver ion transport.[8] The facile reduction of silver phthalazine carboxylate complexes with common PTG developers at room temperature, however, argues against that possibility.[34,35] The role of a toner such as PHZ could be to form a silver complex with a lower redox potential than the original silver source and thereby be reduced more easily [role (3)[15]]. The PHZ could also be directly adsorbed onto the metallic silver surface and therefore direct the deposit of subsequent silver atoms [role (4)]. This latter step is crucial to the control of the metallic silver morphology.

The role of organic species related to Ag surface passivation can be probed directly within a coated film with a

[§]As noted above, PA and its derivatives are used interchangeably in PTG formulations. PA was selected for this model study.

combination of SERS and TEM. The ultimate goal is to control silver morphology. Chemical identification by SERS and direct imaging of both the Ag and its surface passivant by TEM now opens the door for probing the various roles played by organic species in a photothermographic formulation at different stages in the formation of the metallic silver image. Photothermographic formulations contain at least seven different components that have the ability to bond to silver, such as PHZ, 4-MPA, other carboxylates, and aromatic amine-based compounds. It is significant that only PHZ, and to a lesser extent Ag_2(4-MPA), is on the surface even though Butvar and free fatty acid are in high concentration in the D_{max} region. (Free fatty acid has been observed to be a stabilizer for silver nanoparticles).[36,37]

The discovery of PHZ around the dendritic Ag in the Kodak DryView laser imaging film, and around the Ag nanoparticle in the silver nanosol model system, reveals important features about this toner. First, PHZ is capable of displacing such silver ligand "competitors" as 4-MPA (considered a co-toner), fatty acid carboxylates (as reported in a simple thermal decomposition process[36,37]), tetrachlorophthalic acid and even strong silver ligands such as mercaptobenzimidazole. Most interesting is the apparent strong capability of PHZ to adsorb nearly exclusively onto the Ag surface but yet not sufficiently well to completely passivate the nanoparticles, since the nanoparticles still aggregate. Its passivation property is good enough to prevent the aggregates from coalescing, given that the dendritic Ag clusters are now known to be made up of individual Ag nanoparticles and have very large surface areas, Fig. 6. Some aspects of this unique property are revealed by the results on the silver nanosol model system. Those results confirm this organic species to be capable of displacing other adsorbants from the Ag surface, given that silver nanosol is normally well passivated by gelatin. The presence of PHZ apparently destabilizes the surface charge making it possible for the Ag nanoparticles to aggregate into small clumps without coalescing.

Further investigation into how PHZ is bonded to the Ag surface should complement the results shown here. In particular, it would be extremely useful to characterize the surface species at all stages of the silver particle formation during the various stages of the thermal development process, particularly that on the filaments. In this way, compounds may be found that have the ability to further enhance the dendritic silver formation over the filamentary form.

It is worth noting that the diameter of the dendritic Ag cluster is ~100–200 nm, Figures. 5 and 7.[13] By comparison, the size of the Ag aggregates caused by PHZ addition to the Ag nanosol is about 20–200 nm in diameter, Fig. 8. The desired Ag aggregate size distribution for the proper cold and neutral tone in commercial PTG media is a size range spread around an average diameter of 100 nm.[14] Hence the microstructure data indicates that PHZ is a toner that has the ability to passivate Ag nanoparticles and induce aggregation—without coalescence—of Ag clusters in this unique aggregate size range. It should also be noted, however, that there is a key difference between the systems shown here. Dendritic Ag in photothermographic films is spherical, while the aggregated Ag in the nanosol is predominantly linear or branched linear. In either case, PHZ is the only SERS-active species detected on their surfaces. While a direct comparison of the aggregate morphology in the silver nanosol model system to photothermographic media is difficult to make since there are many more components in the latter, the spherical nature of the dendritic Ag appears to suggest that other organic species may be present in the (TEM-detected) passivation shell. The possibility that 4-MPA (considered as a cotoner) may be present to induce a spherical morphology and, hence, minimize the Ag aggregate surface energy, is worth considering. Our findings do suggest that 4-MPA plays an interactive, and not independent, role with PHZ.

We have briefly explored this possible relationship by coating and exposing photothermographic formulations and deliberately leaving out either PHZ or 4-MPA. By comparison to the full-formulation photothermographic formulation, which is processed with a cold tone, neither of the coatings lacking PHZ or 4-MPA developed any images under comparable conditions, and they only showed density at temperatures beyond 150°C (which developed to a yellowish-brown tone).

As can be seen from Table I, under standard processing conditions, there is no optical density in the coatings without PHZ or 4-MPA. By increasing the temperature and time of processing to 145°C/35 sec, the control material completely fogged (D_{min} density is close to D_{max}). However, neither PTG-3 nor PTG-4 show significant optical density. By further increasing the processing temperature to 165°C (35 sec), the PTG-4 (no 4-MPA) becomes completely black (no visible difference between D_{min} and D_{max} areas), the same as the control, while the no PHZ coating density, in PTG-3, is still very low—close to initial D_{min} at standard processing conditions. The interactive nature of the toner (PHZ) with the cotoner (4-MPA) is currently under study.

CONCLUSIONS

For the first time, direct analytical evidence has been obtained that shows the formation of metallic silver nanoparticles within an actual (not model) PTG construction during the late stage of development that is controlled primarily by the surface adsorption of PHZ. Complementary examination and comparison to the effect of PHZ on a silver nanosol model system suggests that PHZ is highly reactive within a limited thermal processing window, but it only partially passivates nanoparticulate Ag. Incompletely passivated surfaces are induced to aggregate but not coalesce. The data reported here suggest that PHZ is the predominant passivant on Ag nanoparticles. The co-toner, PA was not observed directly in this work. However, it is reasonable to infer that the role of PA is to direct the aggregate morphology towards the observed spherical shape. In the absence of PA, liner Ag aggregate chains are produced.

Raman spectroscopy and heavy metal staining, in conjunction with TEM investigation, have provided the initial

evidence for how toners such as PHZ affect the developed silver morphology in a photothermographic construction based on silver carboxylate. We are now in a position to determine what organic compounds are present on various metallic silver morphologies at different stages of thermal development. It is particularly important to establish what is on the first-formed silver filaments in order to understand the filament-to-dendrite transition. Routes to encourage the formation of the dendrites sooner in the development process should provide for improved silver efficiency.

ACKNOWLEDGMENTS

We thank R. J. Meyer (Eastman Kodak Company, now retired) for valuable assistance with RuO_4 staining of various samples used in this report, S. Finn (Eastman Kodak Company) for making the silver nanosol dispersion, and L. Rothberg (Department of Chemistry, University of Rochester) for many helpful discussions.

REFERENCES

[1] P. J. Cowdery-Corvan and D. R. Whitcomb, in *Handbook of Imaging Materials*, edited by A. Diamond and D. Weiss (Marcel Dekker, New York, 2001).
[2] D. R. Whitcomb, *Kirk Othmer Encyclopedia of Chemical Technology*, online edition, 2003. http://www3.interscience.wiley.com/cgi-bin/mrwhome/104554789/HOME.
[3] D. H. Klosterboer, *Imaging Processes and Materials*, Neblette's eighth ed. edited by J. M. Sturge, V. Walworth, and A. Shepp (Van Nostrand-Reinhold, New York, 1989) Chap. 9, pp. 279–291.
[4] D. R. Whitcomb, Photograph. Sci. Photochem. (China) **21**(1), 1 (2003).
[5] V. M. Andreev, E. P. Fokin, Yu. I. Mikhailov, and V. V. Boldyrev, Zh. Nauchnoy i Prikladnoy Fotografii i Kinematografii **24**, 311 (1979).
[6] P. M. Zavlin, A. N. Dyakonov, P. Z. Velinzon, S. I. Gaft, and S. S. Tibilov, Zh. Nauchnoy i Prikladnoy Fotografii **42**, 21 (1997).
[7] M. R. V. Sahyun, J. Imaging Sci. Technol. **49**, 337 (1998).
[8] T. Maekawa, M. Yoshikane, H. Fujimura, and I. Toya, J. Imaging Sci. Technol. **45**, 365 (2001).
[9] P. L. Potapov, D. Schryvers, H. Strijckers, and C. Van Roost, J. Imaging Sci. Technol. **47**, 115 (2003).
[10] S. E. Hill, M. B. Mizen, M. R. V. Sahyun, and Yu. E. Usanov, J. Imaging Sci. Technol. **40**, 568 (1996).
[11] H. L. Strijckers, J. Imaging Sci. Technol. **47**, 100 (2003).
[12] D. R. Whitcomb, W. C. Frank, R. D. Rogers, B. P. Tolochko, S. V. Chernov, and S. G. Nikitenko, *Proc. IS&T 49th Ann. Conf.* (IS&T, Springfield, VA, 1996) p. 426.
[13] S. Chen, T. N. Blanton, D. R. Whitcomb, L. Burleva, and K. A. Dunn, J. Imaging Sci. Technol. **49**, 365 (2005).
[14] D. R. Whitcomb, S. Chen, J. D. Shore, P. J. Cowdery-Corvan, and K. A. Dunn, J. Imaging Sci. Technol. **49**, 370 (2005).
[15] D. R. Whitcomb, M. Rajeswaran, S. Chen, and L. P. Burleva, J. Imaging Sci. Technol. **49**, 394 (2005).
[16] R. K. Chang and T. E. Furtak, *Surface Enhanced Raman Scattering* (Plenum Press, New York, 1982).
[17] K. Kneipp, H. Kneipp, I. Itzkan, R. R. Dasari, and M. S. Feld, J. Phys.: Condens. Matter **14**, R597–R624 (2002).
[18] T. Vo-Dinh, Trends Analyt. Chem. **17**, 557–582 (1998).
[19] E. S. Brandt and T. M. Cotton, in *Physical Methods of Chemistry Volume IXB*, edited by B. W. Rossitor and R. C. Baetzold (Wiley, New York, 1993) pp. 633–718.
[20] Z.-Q. Tian, B. Ren, and D.-Y. Wu, J. Phys. Chem. B **106**, 9464–9483 (2002).
[21] Z. Wang, S. Pan, T. D. Krauss, H. Du, and L. Rothberg, Proc. Natl. Acad. Sci. U.S.A. **100**, 8638–8643 (2003).
[22] D. E. Morel and D. T. Grubb, Polym. Commun. **25**, 68 (1984).
[23] D. Montezinos, B. G. Wells, and J. L. Burns, J. Polym. Sci., Polym. Lett. Ed. **23**, 421 (1985).
[24] I. Geuens, J. Loccufier, and V. Drieghe, European Patent 1431814 (2004).
[25] I. Geuens, J. Loccufier, and V. Drieghe, European Patent 1435298 (2004).
[26] M. C. Lea, J. Am. Sci. **37**, 476 (1889).
[27] C. F. Zou, J. B. Philip, S. M. Shor, M. C. Skinner, and P. Zhou, US Patent 5,434,043 A (1995).
[28] L. D. Peachy, J. Biophys. Biochem. Cytol. **4**, 233 (1958).
[29] D. R. Whitcomb, B. J. Stwertka, S. Chen, and P. J. Cowdery-Corvan, Anal. Chem. (submitted).
[30] D. Montezinos, B. G. Wells, and J. L. Burns, J. Polym. Sci., Polym. Lett. Ed. **23**, 421 (1985).
[31] K. Li, M. I. Stockman, and D. J. Bergman, Phys. Rev. Lett. **91**, 227402-1-4 (2003).
[32] M. Kerker, O. Silman, L. A. Bum, and D.-S. Wang, Appl. Opt. **19**, 3253 (1980).
[33] M. Kawasaki and H. Ishii, Langmuir **11**, 832 (1995).
[34] D. R. Whitcomb and R. D. Rogers, Inorg. Chim. Acta **256**, 263 (1997).
[35] D. R. Whitcomb and R. D. Rogers, J. Chem. Cryst. **25**, 137 (1995).
[36] K. Abe, T. Hanada, Y. Yoshida, N. Tanigaki, H. Takiguchi, H. Nagasawa, M. Nakamoto, T. Yamaguchi, and K. Yase, Thin Solid Films **524**, 327–329 (1998).
[37] S. J. Lee, S. W. Han, H. J. Choi, and K. Kim, J. Phys. Chem. B **106**, 2982 (2002).